The *Drosophila* EcR-Hippo component Taiman promotes epithelial cell fitness by control of the Dally-like glypican and Wg gradient

Colby K. Schweibenz[1,2], Victoria C. Placentra[1,3], Kenneth H. Moberg[1,*]

[1]Department of Cell Biology, Emory University School of Medicine
[2]Graduate Program in Biochemistry, Cell, and Developmental Biology,
[3]Graduate Program in Genetics and Molecular Biology, Emory University

***** Correspondence
kmoberg@emory.edu
Emory University
Department of Cell Biology
615 Michael Street
Atlanta, GA 30322

ABSTRACT

Rapidly dividing cells can eliminate slow growing neighbors through the apoptotic process of cell competition. This process ensures that only high fitness cells populate embryonic tissues and is proposed to underlie the ability of oncogene-transformed cells to progressively replace normal cells within a tissue. Patches of cells in the *Drosophila* wing disc overexpressing the oncogenic Taiman (Tai) transcriptional coactivator kill normal neighbors by secreting Spätzle ligands that trigger pro-apoptotic Toll signaling in receiving cells. However, extracellular signaling mechanisms responsible for elimination of slow growing cells by normal neighbors remain poorly defined. Here we show that slow growing cells with reduced Tai (Tai^{low}) are killed by normal neighbors through a mechanism involving competition for the Wingless (Wg/Wnt) ligand. Elevated Wg signaling significantly rescues elimination of Tai^{low} cells in multiple organs, suggesting that Tai may normally promote Wg activity. Examining distribution of Wg components reveals that Tai promotes extracellular spread of the Wg ligand from source cells across the wing disc, thus ensuring patterned expression of multiple Wg-regulated target genes. Tai controls Wg spread indirectly through the extracellular glypican Dally-like protein (Dlp), which binds Wg and promotes its extracellular diffusion and capture by receptors. Data indicate that Tai likely controls Dlp at two levels: transcription of *dlp* mRNA and Dlp intracellular trafficking. Overall, these data indicate that the Tai acts through Dlp to enable Wg transport and signaling, and that cell competition in the Tai^{low} model arises due to inequity in the ability of epithelial cells to sequester limiting amounts of the Wg growth factor.

INTRODUCTION

The development of an organism is a tightly controlled process, with multiple signaling pathways converging to achieve correct patterning, morphogenesis, and cell fates. As the earliest cells begin to populate tissues, it is advantageous that the fittest progenitors give rise to the entire organism. One example of this is in the formation of the epiblast—early embryonic cells go through a selection process, where more fit cells with higher amounts of pluripotency factors such as TEAD or Myc outcompete cells with a relatively lower dose of these factors[1,2]. This process of pruning unfit cells and selection of fitter cells for survival is known as "cell competition."

The phenomenon of cell competition was first described in the context of *Drosophila melanogaster* cells with defective ribosomal protein function, termed "*Minutes*", that could survive when surrounded by like cells but died in a heterotypic environment mixed with wildtype cells[3]. Cells that die in a heterotypic environment are called "losers," as they undergo apoptosis through mechanisms triggered by neighboring cells termed "winners". A variety of apoptotic mechanism have been proposed to underlie loser fate, including exposure to the pro-apoptotic cytokine Spätzle (Spz) produced by oncogene transformed 'winners'[4-6], non-autonomous induction of autophagy[7,8], loss of apicobasal polarity[9], and inequities in expression of the transmembrane factor Flower[10], the secreted protein SPARC[11], or the Ca^{+2} binding protein Azot[12]. Altering the dose of the dMyc oncogene has also been proposed to generate competitive differences by altering the ability of cells to compete for limiting amounts of the Dpp morphogen[13,14].

In previous work we found evidence that wing cells overexpressing the conserved coactivator and oncogene Taiman (Tai; human AIB/SRC3/NCOA3) kill neighboring cells by

overproduction and secretion of Spz ligands, in particular Spz4[6], which is similar to a proposed mechanism by which excess Myc confers winner status[4]. Intriguingly, *Drosophila* cells with reduced Tai expression are viable, proliferate more slowly than normal cells, and generate small but properly patterned organs [15]. However, they have not been tested for their fitness status, and whether they become losers that resemble cells with reduced levels of the dMyc oncogene (i.e., Myc^{low} cells, as in [4,5]). Here we have used a homozygous viable allele of *tai* that behaves as a weak hypomorph to investigate the role of Tai in cell competition. We find that larval wing disc cells with reduced Tai (Tai^{low}) survive in a homotypic environment but are eliminated by neighboring wildtype cells in a heterotypic environment of clonal mosaics. A genetic screen to identify pathways involved in competitive elimination of Tai^{low} cells identifies alleles of the Wnt/Wg pathway inhibitor *Adenomatous polyposis coli* (*APC*) as suppressors of Tai^{low} elimination, suggesting that Tai^{low} elimination may be due to a deficit of Wg signaling. Examining the Tai-Wg link more closely reveals that Tai is required for formation of the Wg gradient in the larval wing pouch and for patterned activation and repression of Wg target genes at different points along the Wg gradient. We trace this defect to a role for Tai in promoting levels and intracellular trafficking of the Dally-like protein (Dlp) glypican, which binds extracellular Wg and facilities its movement away from source cells. Evidence suggests that Tai is a key determinant of the effect of Dlp on Wg steady-state levels: excess Dlp triggers Wg accumulation in Tai-depleted cells, but triggers Wg loss in cells that also express Tai. Dlp accumulates intracellularly in Tai^{low} clones, confirming a link between Tai and Dlp trafficking. Given that cells lacking *Apc* are 'winners' in the wing pouch and adult intestine[16,17], we propose that Tai regulates competitive status though an underlying developmental role in promoting Dlp-

dependent Wg capture and signaling. As a result, cells with reduced Tai are disadvantage with normal neighbors for capture of limiting amounts of Wg.

RESULTS

Cells with reduced Tai are selectively killed in clonal mosaics

Combining the weak, viable hypomorph *tai*^{k15101} with a deletion (*Df ED678*) that completely removes the second copy of *tai* produces small but normally patterned adults with proportionally smaller organs[15]. Larval wing discs from these *taik15101/Df* animals contain background levels of apoptotic cells (**Fig. 1A-A′,D**) suggesting that wing size reduction is the result of a proliferative deficit rather than surplus apoptosis. This hypothesis is consistent with our previous finding that Tai promotes cell division in the larval wing[15]. Generating boundaries between *tai*^{k15101} cells (*tai*^{k15101}*,FRT40A*) and normal cells (*FRT40A*) using the Flp-FRT mosaic system results in significantly elevated cleaved Dcp-1 (cDCP-1) caspase within *tai*^{k15101} clones (**Fig. 1B-B″, C-C″, D**), indicative of apoptosis. This excess cDcp1 is especially evident in *tai*^{k15101} clones located in the wing pouch, a developing epithelium that is widely used to assess competitive status [4,18]. These data show that pouch cells with one hypomorphic *tai* allele (i.e., *tai*^{k15101}*/Df*) are viable when surrounded by like cells, but that cells with two copies of the *tai*^{k15101} hypomorph die when surrounded by *tai*^{wt} cells. These data indicate the existence of an extracellular competition mechanism that allows normal *tai*^{wt} cells to kill *tai*^{k15101} (hereafter *tai*^{low}) neighbors.

Elimination of *tai*^{low} cells requires Wg, Hippo, and canonical apoptosis pathways

A *mini-w*$^{+}$ minigene present in the *tai*^{k15101} hypomorph generates red pigment that visually marks *tai*^{low} heterozygous or homozygous cells in the adult eye. As in the larval wing disc, *tai*^{k15101}*/Df* cells readily populate an adult eye composed of alike cells, but patches of *tai*^{low} cells form small clones when placed in competition with control (*white*$^{-}$*;FRT40A*) cells using an eye-specific

Flpase transgene (*eyFLP*) (**Fig. 2A-B**). By comparison, cells carrying a *mini-w*$^{+}$ marked *FRT40* chromosome occupy approximately 50% of the adult eye.

To identify genes and pathways involved in elimination of *tai*^{low} eye cells, a collection of mutant alleles of candidate competition factors (**Supplemental Table 1**) were screened for dominant rescue of *tai*^{low} small clone size in the adult eye (**Fig. 2C-H**). This approach yielded 'hits' in the pro-apoptotic Rpr-Hid-Grim (RHG) factors (*hid*^{1} and the *H99* deletion), the Hippo pathway kinase *warts* (*wts*^{1}), and the Wg pathway inhibitor *Adenomatous polyposis coli* (*Apc*^{MI01007}). Alleles affecting components of the Spz-Toll, IMD, or ecdysone pathways did not obviously modify *tai*^{low} clone size, nor did alleles of other candidate factors such as the transmembrane proteins *flower* and *Sas*, the transcription factors *p53* and *Xrp1*, the autophagy factor *Atg1*, and the secreted glycoprotein *Sparc* [8-11,19-22] (data not shown). These genetic data confirm separate elements of *tai*^{low} loser fate: rescue by *hid*^{1} and *H99* provide genetic evidence that elimination of *tai*^{low} cells requires the canonical RHG-Diap1-Caspase pathway (rev. in [23]), while rescue by *wts*^{1} is consistent with Tai protecting against the "loser" fate through Yorkie, which is bound by Tai and phosphorylated by Wts[15,24,25]. By contrast, *tai*^{low} rescue by *Apc* suggests an unexpected link between Tai competitive status and Wg signaling. A second *Apc* mutation (*Apc*^{Q8}) in combination with an inactivating allele in its paralog *Apc2* (*Apc2*^{N175A}) similarly increases survival of *tai*^{low} cells in the eye (**Fig. 2H**).

The larval wing pouch is bisected along the D-V (dorsoventral) midline by a stripe of Wg-expressing cells that generate mirror image gradients (dorsal and ventral) that guide wing growth and patterning[26]. Quantification of *tai*^{low} clone size within the larval wing pouch at 50hrs post induction (*hsFlp*) indicates that *RHG*, *wts*, or *Apc/Apc2* alleles recovered in the eye screen also increase the size of *tai*^{low} pouch cells (**Figure 3A-H**), with *H99* and the compound

Apc^{Q8},*Apc2*^{N175A} allele having the largest effects. *H99* and *Apc* alleles also enhance recovery of 76hr old *tai*^{low} clones, which are normally eliminated by this time point (**Fig. S1**). Together, these data indicate that competitive elimination of *tai*^{low} cells requires RHG proteins and can be attenuated by derepressing the Wg or Hippo pathways.

Tai modulates transcription of Wg-regulated genes and formation of the Wg gradient

The extended survival of 76hr *tai*^{low} clones in *Apc* and *Apc,Apc2* heterozygous backgrounds imply a relatively strong link between Tai and Wg signaling. To test sensitivity of Wg pathway activity to Tai dosage, *UAS* transgenes were used to test whether *tai* overexpression or reduction affects transcription of two Wg target genes: *naked cuticle* (*nkd*), a mid-threshold target of the Wg gradient that is expressed in bands of cells on either side of the DV midline[27] (*nkd-lacZ*), and *wg* itself, which is repressed by an autoinhibition loop that refines *wg* transcription to a narrow stripe at the DV midline[28] (*wg-lacZ*). Tai overexpression (*en>tai*) expands *nkd-lacZ* expression into dorsal and ventral domains that correspond to distal tails of the Wg gradient and normally express low *nkd* (**Fig. 4A-A", B-B″,** see brackets, and **4D-E**). Tai depletion strongly retards *nkd-lacZ* in regions close to the DV midline that normally receive high Wg (**Fig. 4C-C″, D-E**). Examining *wg* transcription with the *wg-lacZ* transgene shows that *tai* RNAi (*enGal4*) causes *wg-lacZ* to spread dorsally and ventrally away from the DV margin (**Fig. 5B-B′**, see arrow), while reciprocally elevating *tai* has little effect on *wg* transcription (**Fig. 5C-C′**). These data are consistent with Tai acting as a positive upstream regulator of Wg signaling in pouch cells, such that activation of *nkd* and autoinhibition of *wg* each fail when Tai is removed.

Failure to constrain *wg-lacZ* activity to DV margin cells in Tai-depleted discs (see **Fig. 5B′**) resembles the effect of mutations that block receipt of the Wg ligand[28]. Examination of the Wg gradient in pouch cells with reduced Tai in the posterior domain (*en>tai* RNAi) detects robust

Wg in source cells but significant reduction in Wg spreading into the dorsal and ventral pouch (**Fig. 6A** vs. **6C**, arrows). This loss of the Wg gradient occurs despite expansion of the *wg* expression domain in Tai RNAi pouches (see **Fig. 5B-B′**). Overexpression of Tai produces gaps in the stripe of Wg protein in DV cells (**Fig. 6B**, arrows) that also does correlate with a loss of *wg* transcription (see **Figs. 5C-C′**), suggestive of a post-transcriptional effect of excess Tai on Wg stability, uptake, or trafficking in the DV regions. Quantification of anti-Wg staining intensity confirms that Tai RNAi blocks formation of the Wg gradient and indicates that Tai overexpression elevates Wg in regions further from the DV margin (**Figs. 6D-E**). Considered together, these data are consistent with a requirement for Tai in forming the Wg gradient by control of Wg protein extracellular diffusion and/or internalization and turnover.

Tai is required for expression of Dally-like protein, a glypican required for Wg signaling

The GPI-anchored glypican Dally-like protein (Dlp) binds lipidated Wg and facilitates its extracellular diffusion and capture by Frizzled receptor[29-33]. Notably, homozygous loss of *Apc* produces competitive 'winners' by upregulating the secreted enzyme, Notum, which then cleaves Dlp and deprives normal neighbors of the ability to sequester or sense Wg[17]. Given that *Apc* heterozygosity rescues tai^{low} elimination, *tai* alleles were tested for modulation of Dlp levels in the larval pouch. Excess Tai significantly elevates Dlp protein among posterior cells (*en>tai*) and Tai depletion had the opposite effect of depleting Dlp (**Figs. 7A-C** and graphs in **7D-E)**. Expression of the Dlp-related glypican Dally[34] also rises upon Tai overexpression but is insensitive to Tai depletion (*dally-lacZ*; **Figs. S2A-C**), other than shrinkage of the *dally-lacZ* pattern due to reduced Posterior (P)-domain size due to Tai loss (arrows **Figs. S2A′** vs. **S2C′**). These data indicate that Tai is rate-limiting for Dlp expression in the pouch and may be able to induce *dally* expression when overexpressed.

Examining Dlp dynamics further, we find that RNAi depleting the extracellular protein Pentagone, which promotes Dlp/Dally glypican internalization and turnover[34], produces little change in Dlp levels among Tai-depleted cells (**Fig. S3A-C**, see bracketed regions). RNA-seq analysis of Tai-expressing wing discs detects elevated *dlp* mRNA, indicating that Tai may control *dlp* mRNA abundance (**Fig. S4)**. Consistent with this hypothesis, EcR CUT&RUN analysis [35] in 3rd instar larval wing discs detects EcR binding peaks on the *broad* and *dlp* loci; *dlp* is flanked by two EcR peaks with another located in a *dlp* intron (**Fig. S4**). Orthogonal slices that traverse the Wg stripe of *en>tai* discs from control (anterior) to Tai overexpressing (posterior) regions confirm that Tai overexpression lowers Wg protein levels (**Fig. S5**). Notably, expression of a *dlp* transgene causes Wg accumulation on the DV flanks of Tai-depleted wing discs (**Fig. 7E-E′**), indicating that *tai* RNAi cells are similar to *wt* cells and retain Wg when provided extra Dlp[31]. However, expression of *dlp* together with *tai* (*en>tai,dlp*) has a reciprocal effect of enhancing Wg loss protein at the DV margin (**Fig 7F-F′**) and Wg build-up on the dorsal hinge (asterisk in **7G′**). Given that Tai expression with the same driver (*en>tai*) elevates Wg transcriptional output across the pouch (see **Figs. 4-5**), this loss of Wg may be due to enhanced trafficking and/or uptake. These data suggest that Tai status determines the effect of excess Dlp on Wg levels: Dlp depletes Wg levels across the pouch cells when excess Tai is present but retains Wg in Tai-depleted cells. A reciprocal test of a Dlp role in Tai overexpressing discs indicates that two different *dlp* RNAi lines do not rescue gaps in the Wg stripe that appear with Tai-overexpressing (arrows, **Fig. S6A-D**). These data indicate that Tai status determines the effect of excess Dlp on Wg, but that excess Tai may engage a different mechanism to modulate Wg protein in DV margin cells.

In the course of these analyses, we noted that wild type Tai or a version of the protein lacking PPxY motifs required to bind Yki [15] (Tai^{PPxA}) drive accumulation of Dlp protein across the pouch (*enGal4*) (**Fig. S7A-B**) including in the DV midline region where Dlp is normally excluded (e.g., see arrows in **Fig. 7A**). Under normal circumstances, Dally is expressed in this region (e.g., see **Fig. S2**) and promotes short range Wg signaling from source cells[36]. Consistent with this local dependence on Dally, Tai-depletion only in DV midline cells with a wing margin driver (*big bang (bbg)-Gal4*) has only a mild effect on distribution of Wg protein; however, providing exogenous Tai to these cells broadens the Wg-positive domain (**Fig. 8A-C**). Given that Tai does not elevate *wg* transcription (see **Fig. 5C**), this finding indicates that overexpressing Tai in DV midline cells is sufficient to enhance local spread of Wg protein and increase abundance of Wg-positive puncta (in **Fig. 8B′**) which have been shown to correspond to secretory vesicles[37]. Thus, expression of Tai in source cells enhances Wg secretion, while expression in the DV flanks can cooperate with excess Dlp to deplete Wg across the Posterior (P) -domain.

Dlp protein is altered in *tai^{low}* clones

Relative to the lethal *tai* RNAi transgene (e.g., with *actin5c-Gal4*[38]), the viable *tai^{low}* allele is predicted to yield correspondingly weaker phenotypes. To improve recovery of comparatively rare *tai^{low}* pouch clones, *hsFlp* was applied in the *H99/+* background (see **Fig 3**). In this configuration, *tai^{low}* pouch clones contain elevated levels of Dlp relative to adjacent control cells (arrows, **Fig. 9A-A″**). This result suggests that *tai^{low}* could perturb Dlp intracellular traffic, either during secretion or internalization. To test this model, Dlp was reanalyzed in *tai^{low}* clones under conditions that do not permeabilize membranes; this approach detects only basal levels of Dlp on the surface of control and *tai^{low}* disc cells (**Fig. 9B-B″**). Indeed, closer inspection of *tai^{low}* hypomorphic clones in tangential slices indicates that Dlp is mislocalized to the cytoplasm (**Fig.**

9C-D). Given that removing Pent, which stimulates Dlp internalization[34], does not rescue Dlp loss in Tai RNAi cells, Tai may promote both *dlp* mRNA expression and Dlp protein secretion, and that the consequent decline in ability to compete for Wg with normal neighbors deprives *tai*^{low} cells of a signal necessary for growth and survival.

DISCUSSION

Here we show that cells with a reduced dose of the Tai coactivator, which functions in the ecdysone and Hippo pathways[15,39], are killed by normal neighbors through a mechanism involving competition for the Wingless (Wg/Wnt) ligand. Elevated Wg signaling significantly rescues elimination of Tai^{low} cells in multiple organs, suggesting that Tai may normally promote Wg activity. Examining distribution of Wg components reveals that Tai promotes extracellular spread of the Wg ligand from source cells across the wing disc, thus ensuring patterned expression of multiple Wg-regulated target genes. Tai controls Wg spread indirectly through the extracellular glypican Dally-like protein (Dlp), which binds Wg and promotes its extracellular diffusion and capture by receptors. Data indicate that Tai likely controls Dlp at two levels: transcription of *dlp* mRNA and Dlp intracellular trafficking. Overall, these data indicate that the Tai acts through Dlp to enable Wg transport and signaling, and that cell competition in the Tai^{low} model arises due to inequity in the ability of epithelial cells to sequester limiting amounts of the Wg growth factor.

One key conclusion from these data is the mechanism through which Tai^{high} cells kill normal neighbors (e.g., through Spz-Toll)[6] is distinct from the mechanism that eliminates Tai^{low} cells. The former mechanism is produced by triggering an innate immune pathway and may require priming by chronic microbial infection[18], while the latter derives from a developmental role in Dlp-mediated Wg diffusion and turnover (this study). These mechanisms may both occur

in vivo, although in different contexts, with Tai^{high} overexpression mimicking oncogene activation in cancer, and Tai^{low} representing cells in developing tissues that receive weaker proliferative or survival signals than neighbors. In the developing wing disc, gradual scaling of the Wg gradient as the tissue grows ensures that adjacent cells experience only incremental changes in concentration of pro-growth morphogens[40]. Artificially steepening of a gradient, as occurs in *pent* mutant wing discs[21], or creating patches of cells deficient in morphogen capture (e.g., with *tai*^{low} or *tai*^{RNAi}) or signaling (e.g., as in Wg pathway mutants[17]) within an otherwise intact gradient each create sharp differences in morphogen activity. This model is supported by the finding that artificial boundaries between glypican expressing and non-expressing cells is sufficient to induce cell competition among *Drosophila* follicle stem cells[41]. Intriguingly, *dlp* follicle clones are 'winners' while *dally* clones are 'losers', which implies different roles for Wg in survival of pouch cells vs. follicle stem cells.

The finding that *tai* alleles perturb Dlp expression, retard the Wg gradient, and interact with *Apc* alleles in eye and wing epithelia seems to suggest that Tai gain and loss phenotypes in these tissues may be driven in part by changes in Wg signaling. It remains to be determined whether Tai acts broadly across multiple tissues and developmental stages to modulate Wg, or whether this role is limited to specific cell types. As Tai is a transcriptional coactivator it is likely to mediate its Wg regulatory effects through other factors that directly contact DNA. The identity of this factor(s) is unclear. One candidate is the ecdysone receptor EcR, which brings Tai into a transcriptional regulatory complex whose components are conserved across metazoans (i.e., ERα-NCOA3-p300)[42]. The role of EcR in innate immune transcription[43] is consistent with our finding that EcR is involved in intertissue invasion led by Tai^{high} cells[6]. However, the role of an EcR-Tai complex in death of Tai^{low} cells has not been examined. Ecdysone can promote (or

‘gate’) activity of both major morphogen gradients in the wing disc[44], and the presence of EcR CUT&RUN peaks in the *dlp* genomic region (see **Fig. S4**) seems to imply EcR may have some role in Dlp expression. EcR can also repress *wg* transcription in areas of the pouch[4 5], much as we have found that Tai represses *wg* transcription on either side the DV margin (see **Fig. 5B**). However further work is required to determine whether either of these roles requires an EcR-Tai complex. Mild rescue of tai^{low} elimination by a *wts* allele indicates that slight elevation of Yki activity can promote tai^{low} survival. However, the ability of the non-Yki binding form of Tai, Tai^{PPxA}, to efficiently induce Dlp accumulation in pouch cells is not consistent with a requirement for Tai to bind Yki during the competition process. Alternatively, Tai may modulate Wg signaling independent of interactions with EcR and Yki, perhaps through other transcription factors. Determining Tai-binding partners involved in regulation of the Wg pathway and establishing Tai transcriptional targets whose products modulate secretion and/or endocytosis of glypicans could yield broad insight into mechanisms that calibrate morphogen diffusion in development and disease.

Lead contact and resource availability

Requests for resources and reagents should be directed to and will be fulfilled by Lead Contact (kmoberg@emory.edu).

Acknowledgements

We thank the Emory Integrated Cellular Imaging Core for their expertise and assistance. We also thank E. J. M. Storkebaum, the Developmental Studies Hybridoma Band (DSHB), Bloomington Drosophila Stock Center (BDSC), the Harvard Transgenic RNAi Project (TRiP), and the Vienna Drosophila Stock Center for antibodies and stocks. We also thank members of Moberg laboratory for their helpful discussion. This work was funded by NIH T32 GM008367-30, NIH F31 Predoctoral Fellowship CA254207 (CKS), and NIH R01 GM121967 (KHM)

Author Contributions

Conceived and designed the experiments: CKS, KHM. Performed the experiments: CKS. Analyzed the data: CKS, VCP, KHM. Authored the paper: CKS. Edited the manuscript: CKS, KHM. Funding and Acquisition: CKS, KHM.

Materials and Methods

Drosophila culture

Fly stocks were maintained under standard culture conditions at 25ºC, 12 hr light:dark cycles in humidity-controlled incubators. Experiments used a mix of female and male animals. All crosses were maintained on standard molasses food supplemental with yeast. Unless specified, flies were mated and allowed to lay eggs for a period of 24-48 hours, and then dissected at wandering third instar. Lines used are referred to in **Key Resources Table** (BDSC stock numbers indicated).

Strategy for randomization and/or stratification

Animals of both sexes were used for experiments. A minimum of 10 total imaginal wing discs over three biological replicates were used in all experiments. Figures presented are representative images of each genotype.

Adult eye screen

Adult females were aged for three days to allow condensation of pigment granules then frozen at -20ºC for >5 minutes before imaging with a Nikon SMZ800N microscope at 25X magnification (2.5X objective x 10X eyepiece) using a Leica MC170HD camera and a Nii-LED High intensity LED illuminator. Flies were submerged in 70% ethanol to eliminate glare. Multiple focal planes were imaged and merged in Photoshop to generate a final image.

Cell Competition Assays

Mated flies were allowed to lay for 24 hrs before flipping into a new vial. 48-50 hrs after egg lay (AEL), FLP recombinase was induced by heat-shocking of the larvae at 37ºC for about one hour, except for in the generation of "Flp-out" clones where larvae were heat-shocked for 1.5 hrs. Third instar larvae were then dissected at 96 hrs AEL. Both male and female larvae were dissected. Clonal areas were measured using ImageJ, and only clones in the wing pouch were considered for analysis.

Immunofluorescence and microscopy

Immunofluorescence and microscopy were performed using standard methods. Briefly, wing discs were dissected in 1X phosphate-buffered saline (PBS), fixed for 20 minutes in 4% paraformaldehyde (PFA) at room temperature (RT), rinsed 5X in 1X PBS, and then permeabilized with 1X PBS and 0.3% Triton X-100 (0.3% PBST). For extracellular stain without permeabilization, the protocol was performed as in [46]. Discs were then blocked with 10%

normal goat serum (NGS) and then incubated in diluted primary antibody containing 10% NGS and 1X PBS and 0.1% Triton X-100 (0.1% PBST). Samples incubated in primary antibody solution at 4ºC overnight, washed 5X with 0.1% PBST, incubated with DAPI (1:500) for 5 minutes, washed 3X with 0.1% PBST, and then incubated for 1 hr at RT with secondary antibody solution diluted with 10% NGS and 0.1% PBST. Discs were then washed 5X times with 0.1% PBST and incubated in n-propyl gallate (NPG, 4% w/v in glycerol) overnight. Discs were mounted in NPG on glass coverslips and then imaged with a Nikon A1R confocal system using 20X and 40X objectives. Images were processed with Fiji, Photoshop, and Illustrator software. ImageJ was used for clonal area measurements. Refer to **Key Resources Table** for full list of antibodies, dilutions, and other reagents used.

Fluorescence intensity analysis

Fluorescence intensities were measured across equal regions of interest (ROIs) using Image J/Fiji. Briefly, the ROI was positioned such that it was: 1) centered over the AP boundary as defined by the *en>GFP* control channel, 2) below the DV line (approximately halfway between the DV boundary and the bottom of the pouch), and 3) extended approximately halfway into each compartment (anterior and posterior). Raw fluorescence intensity values were standardized such that the mean anterior fluorescence was equal to 1, and posterior fluorescence was relative to anterior. Analyses and fluorescence intensity plots were performed and created in R (R version 4.1.1 (2021-08-20)). Posterior: anterior mean fluorescence intensity ratios were plotted, and statistics performed using GraphPad Prism. Unpaired t-tests with Welch's corrections were performed.

Quantitation and Statistical Analyses

Unpaired Student's t-tests or one-way ANOVAs (GraphPad Prism) were used to analyze significance between datasets. Significance was considered to be $p<0.05$. Normal distributions were assumed.

KEY RESOURCES TABLE

REAGENT or RESOURCE	SOURCE	IDENTIFIER
Antibodies		
Mouse anti-β-Gal (1:100)	Promega	Z3781; RRID: AB_430877
Rabbit anti-Dcp1 (1:100)	Cell Signaling	9578; RRID: AB_2721060
Mouse anti-Wg (1:50)	DHSB	4D4; AB_528512
Mouse anti-Dlp (1:50)	DHSB	13G8; AB_528191
Goat anti-mouse-Cy3 (1:50)	Jackson ImmunoResearch	115-166-003; RRID: AB_2338683
Goat anti-mouse-Cy5 (1:50)	Jackson ImmunoResearch	115-175-146; RRID: AB_2338712
Goat anti-rabbit-Cy3 (1:50)	Jackson ImmunoResearch	111-165-003; RRID: AB_2338000
Goat anti-rabbit-Cy5 (1:50)	Jackson ImmunoResearch	111-175-144; RRID: AB_2338013
Chemicals, peptides, and recombinant proteins		
Triton X-100		
20% Paraformaldehyde	Electron Microscopy Sciences	15713
Trizol	Invitrogen	15596018
DAPI	Invitrogen	D1306
Normal goat serum (NGS)	Jackson ImmunoResearch	005-000-121
n-propyl gallate (NPG)	Sigma	P-3130
Experimental models: Organisms/strains		
D. melanogaster: tai^{k15101}	BDSC	93042
D. melanogaster: tai^{k15101}*, FRT40A*	This study	N/A
D. melanogaster: FRT40A	BDSC	5758
D. melanogaster: hsflp; FRT40A,ubiGFP	BDSC	Constructed from component stocks
D. melanogaster: eyflp; FRT40A,ubiGFP	BDSC	Constructed from component stocks
D. melanogaster: tai^{PPxA}*, FRT40A*	S. Verghese, Emory University	N/A
D. melanogaster: Df (3L) H99 (hid, reaper, grim)	BDSC	1576
D. melanogaster: Df (2L) ED678 (tai)	BDSC	8906
D. melanogaster: UAS-tai (III)	BDSC	6378

D. melanogaster: UAS-RFP (II)	BDSC	30556
D. melanogaster: UAS-RFP (III)	BDSC	31417
D. melanogaster: UAS-tai-IR	BDSC	28971
D. melanogaster: UAS-taiPPxA	Moberg lab stock	Zhang et al, 2015 *Dev Cell*
D. melanogaster: UAS-wg	BDSC	5918
D. melanogaster: UAS-wg-IR	BDSC	32994
D. melanogaster: UAS-dlp	BDSC	9160
D. melanogaster: UAS-dlp-IR	BDSC	34089
D. melanogaster: UAS-dlp-IR	BDSC	34091
D. melanogaster: UAS-yki-IR	VDRC	104523
D. melanogaster: UAS-magu-IR	BDSC	51169
D. melanogaster: nkd-lacZ	BDSC	25111
D. melanogaster: wg-lacZ	BDSC	11205
D. melanogaster: hid^{1}	BDSC	631
D. melanogaster: Toll^{rv18} *(Toll-1)*	BDSC	30913
D. melanogaster: Tollo^{1} *(Toll-8)*	BDSC	36549
D. melanogaster: crb^{8F105}	BDSC	7099
D. melanogaster: Oatp74D^{BG0653} *(EcI)*	BDSC	12430
D. melanogaster: sas^{15}	BDSC	2098
D. melanogaster: p53$^{11-1B-1}$	BDSC	6816
D. melanogaster: Atg1^{3}	BDSC	60732
D. melanogaster: scrib^{dt14}	BDSC	29014
D. melanogaster: Apc^{MI01007}	BDSC	34138
D. melanogaster: Apc^{Q8}*Apc*^{N175K}	BDSC	7211
D. melanogaster: sd^{12}	BDSC	9371
D. melanogaster: SPARC^{MI00329}	BDSC	30711
D. melanogaster: wts^{x1}	BDSC	44251
D. melanogaster: Df (3R) BSC491 (SPE)	BDSC	24995
D. melanogaster: PGRP-LB^{4}€	BDSC	55715

D. melanogaster: p53$^{11\text{-}1B\text{-}1}$	BDSC	6816
D. melanogaster: Xrp1^{KO}	E. Storkebaum, Donders Institute	N/A
D. melanogaster: spz^{4} *Rel*^{E20}	BDSC	55718
D. melanogaster: ilp8KO	P. Leopold, Institut Curie	Boone et al, 2016 *Nat Commun*
D. melanogaster: fweDB25	BDSC	51996
D. melanogaster: UAS-EcRLBD	Wardwell-Ozgo, J. Emory University	Wardwell-Ozgo et al, 2023, *bioRxiv*
D. melanogaster: UAS-EcRLBD-A483T	Wardwell-Ozgo, J. Emory University	Wardwell-Ozgo et al, 2023, *bioRxiv*
Software and algorithms		
ImageJ	Open source	https://imagej.net/software/fiji/
Prism	GraphPad	https://www.graphpad.com/
Photoshop	Adobe	https://www.adobe.com/products/photoshop.html
Illustrator	Adobe	https://www.adobe.com/products/illustrator.html
R Studio	Open source	https:/r-project.org

Figure Legends

Figure 1. *tai*^{low} cells survive in a homotypic environment but die in a heterotypic environment. (A-A′) 3rd larval instar *tai*^{k15101}*/Df(2L)ED678* wing disc stained with anti-cleaved Dcp-1 (cDcp1; red) and nuclei (DAPI; blue). (**B-C**) *hsFlp* generated clones of control *FRT40A* (**B-B″**) or *tai*^{k15101}*,FRT40A* (**C-C″**) cells marked by the absence of GFP (green) and co-stained for cDcp-1 (red) and nuclei (DAPI; blue). Magnified insets are provided. **(D)** Quantification of cDcp-1 in *tai*^{k15101}*/Df(2L)ED678* heterotypic discs or *tai*^{k15101} clones calculated by percent Dcp1-positive area/total clone area (Student t-test, p <0.0001).

Figure 2. Modification of *tai*^{low} clone survival in the adult eye. Adult female eyes of the indicated genotypes: (**A**) *tai*^{k15101}*/Df(2L)ED678*; (**B-C**) *eyFLP* mosaic eyes with *w-;FRT40A* flipped over (**B**) *tai*^{k15101}*,FRT40A* or (**C**) *FRT40A,m-w*$^{+}$; (**D-H**) *eyFLP* mosaic eyes with

tai^{k15101}*;FRT40A* flipped over *FRT40A,m-w*$^{+}$ in the background of (**D**) *hid*^{1}, (**E**) *Df(3L)H99*, (**F**) *wts*^{x1}, (**G**) *Apc*^{MI01007}, or (**H**) *Apc2*^{N175K}*,Apc*^{Q8}.

Figure 3. Alleles from the eye screen also modify *tai*^{low} clone survival in L3 wing pouch

(**A-G**) Larval wing discs bearing *hsFlp/FRT*-generated 50hr-old *tai*^{low} clones (GFP-negative) either (**B**) alone, or in the background of the indicated alleles (**C-G**). Twinspots appear brighter due to two copies of *GFP*. **(H)** Quantification of *control*(*FRT40A*) or *tai*^{low} size ratio (area ratio of clone:twin-spot) alone (-) or in the indicated genetic backgrounds.. ****p <0.001, ***p= 0.0003, *p = 0.0157, *ns* = not significant (One-way ANOVA with Dunnett post hoc test).

Figure 4. *tai* promotes expression of the Wg pathway reporter *nkd-lacZ*. (**A-C**) Expression of the *nkd-lacZ* reporter (greyscale) in (**A-A″**) *control* (*en>GFP,RFP*), (**B-B″**) Tai overexpressing (*en>tai,GFP*), or (**C-C″**) Tai-depleted larval wing discs. **(D)** Relative anti-ßGal fluorescence intensity on either side of the A-P boundary among pouch cells located just below the D/V boundary. **(E)** Mean relative fluorescence intensity plotted as a ratio of posterior to anterior intensity. *RFP* vs *tai* *p=0.0004; *RFP* vs *tai*^{RNAi} *p<0.0001 (Unpaired student t-test with Welch's correction).

Figure 5. Tai is required for the auto-inhibitory loop that refines *wg* transcription. (A-C) Expression of the *wg-lacZ* reporter in *enGal4* larval wing discs as detected by anti-ßGal staining (white in **A-C**, black in **A′-C′**) in *control* RFP (**A**), Tai-depleted (**B**), or Tai overexpressing (**C**) discs. Arrow in **B′** indicates failure to refine *wg-lacZ* to the DV boundary in P-domains depleted of Tai.

Figure 6: Tai is required for formation of the Wg gradient. Wg protein (greyscale) in (**A-A″**) *control* (*en>GFP,RFP*), (**B-B″**) Tai overexpressing, or (**C-C″**) Tai-depleted larval wing discs. *enGal4* activity in the P-domain is marked by GFP. Arrows in **B′** mark gaps in Wg DV stripe characteristic of Tai overexpression. Arrows in **C′** mark the clear drop in total Wg on the DV flanks of P-domains depleted of Tai. **A″-C″** provide higher magnification views of regions in **B′-C′. (D)** Relative Wg fluorescence intensity of pouch cells below D/V boundary (to avoid Wg source cells) plotted from anterior to posterior. **(E)** Mean Wg relative fluorescence intensity plotted as a ratio of posterior to anterior intensity. *RFP* vs *tai* **p*=0.0443, *RFP* vs tai^{RNAi} **p*<0.0156 (Unpaired student t-test with Welch's correction).

Figure 7: Tai controls Dally-like protein (Dlp) levels. (A-C,F-G) Anti-Dlp staining (greyscale) in (**A-A″**) *control* (*en>GFP,RFP*), (**B-B″**) Tai overexpressing (*en>tai,GFP*), and (**C-C″**) Tai-depleted cells. Arrows in **A′** mark Dlp exclusion from the DV boundary region. Overexpression of Dlp restores Wg in Tai-depleted cells (**F-F′**; see arrow in magnified view), but causes complete loss of the Wg DV stripe in Tai overexpressing disc regions (**G-G′**; see arrow in magnified view). **(D)** Relative Dlp fluorescence intensities of pouch regions below D/V boundary plotted from anterior to posterior. **(E)** Mean relative Dlp fluorescence intensity plotted as a ratio of posterior to anterior intensity. *RFP* vs *tai* **p*=0.0008, RFP vs tai^{RNAi} **p*=0.0002 (Unpaired student t-test with Welch's correction).

Figure 8: Tai expression at the D/V boundary enables excessive Wg spread. (**A-C**) Anti-Wg signal (greyscale) in **(A-A′)** control (*bbg>RFP*), (**B-B′**) Tai-overexpressing (*bbg>tai*), or Tai-

depleted (**C-C′**) discs co-stained for nuclei (DAPI; blue). Dotted lines denote magnified views of Wg in **A′-C′**.

Figure 9: The *tai*^{low} hypomorph causes Dlp intracellular accumulation in pouch cells. (**A-D**) *hsFlp* generated *tai*^{low} clones (GFP negative) in a *H99/+* background co-stained for Dlp (greyscale) and nuclei (DAPI; cyan). Discs in panels **A-A″** and **C** were permeabilized to detect total Dlp (intracellular and extracellular), while discs in panel **B-B″** were processed without permeabilization and only detect extracellular Dlp. Arrows in **C** and **D** denote *tai*^{low} cells in side-view with intracellular Dlp.

Supplemental Figure Legends

Figure S1. *H99* and *Apc* alleles allow *tai*^{low} cells to survive 76hrs after clonal induction. Wing discs bearing 76hr old (post-hs) pouch clones of **(A)** *FRT40A* cells or (**B-G**) *tai*^{low} cells in the indicated genetic backgrounds. Clones are GFP-negative and twinspots are bright green. (**H**) Clone:Twinspot area ratios (pixels) of the same genotypes as in **A-G.** Note significant rescue of *tai*^{low} survival by *H99* and *Apc* heterozygosity. ****p <0.001 ***p = 0.0007, ns = not significant (One-way ANOVA with Dunnett post hoc test).

Figure S2. *dally* does not respond to Tai depletion but can be induced by excess Tai. (**A-C**) Expression of the *dally-lacZ* reporter detected by anti-ßgal stain (greyscale) in (**A-A″**) *control* (*en>GFP,RFP*), (**B-B″**) Tai overexpressing (*en>tai,GFP*), or (**C-C″**) Tai-depleted (*en>tai*^{RNAi}*,GFP*) discs. Arrows in **A′** and **C′** indicate shrunken pattern of *dally-lacZ* expression in a Tai-depleted Posterior (P)-domain.

Figure S3. RNAi of Pent, which promotes Dlp internalization, does not fully restore Dlp in Tai-depleted disc regions. Anti-Dlp signal in (**A-A″**) control (*en>GFP*), (**B-B″**) Tai-depleted (*en>tai*^{low}) discs, or discs (**C-C″**) co-depleted for Tai and Pent (*en>tai*^{RNAi}+*pent*^{RNAi}). Brackets denote P-domain with Dlp depletion with *tai* RNAi.

Figure S4. Evidence of *dlp* transcription regulated by Tai. Top (A): IGV traces of RNA-seq reads from *control* (green; *en>GFP*) and Tai-expressing (red; *en>tai*) larval wing discs laid over (**middle-B**) a genomic map of the *dlp* region. **Bottom (C)**: EcR-association peaks in the *dlp* region (published in [35]).

Figure S5. Excess Tai downregulates Wg levels within source cells at the DV margin. Wg signal (greyscale) in a Tai overexpressing disc (*en>tai,GFP*) imaged *en face* (**A-A′**) and (**B-B′**) tangential slices corresponding to **region 1** and **region 2 in** magnified view **(B-B′**). Panel **C** and associated **regions 1** and **1** show equivalent analysis in control (*en>GFP,RFP*) discs.

Figure S6. RNAi depletion of Dlp is not sufficient to block the Tai-induced gaps in the DV stripe of Wg. Wg signal (greyscale) in wing discs expressing either of two *dlp* RNAi constructs alone (#1 or #2 in **A-B**) or in combination with Tai overexpression (**C-D**). Arrows in **C'** and **D'** mark gaps in the Wg stripe.

Figure S7. Tai^{PPxA} is able to induce Dlp expression in the midline region. Dlp signal (greyscale) in (**A-A″**) *control* (*en>GFP,RFP*) or (**B-B″**) Tai^{PPxA} expressing (*en>tai^{PPxA},GFP*) discs. Yellow arrows in **A′** mark Dlp exclusion from cells in either side of the DV margin; arrow in **B′** points to excess Dlp filling this region.

Supplemental Table 1: A genetic screen reveals dominant modifiers of *tai^{low}* cell death. Heterozygous candidate alleles selected from various pathways were placed in the background of a mosaic *eyFlp; Tai^{low}* eye, and positive screen "hits" were determined based on increased recovery of Tai^{low} clones (orange). An allele of *hid*, as well as the *H99* deletion (*reaper, hid, grim*) enhanced recovery of Tai^{low} cells. Other suppressors included *wts^{x1}*, a loss of function allele of the core Hippo pathway kinase and an allele of *Adenomatous polyposis coli* (*Apc*), a key inhibitor of the conserved Wg/Wnt pathway. Refer to Key Resources Table for information about alleles used.

Bibliography

1. Claveria C, Giovinazzo G, Sierra R, Torres M. Myc-driven endogenous cell competition in the early mammalian embryo. Nature. 2013;500(7460):39-44. Epub 20130710. doi: 10.1038/nature12389. PubMed PMID: 23842495.
2. Hashimoto M, Sasaki H. Epiblast Formation by TEAD-YAP-Dependent Expression of Pluripotency Factors and Competitive Elimination of Unspecified Cells. Dev Cell. 2019;50(2):139-54 e5. Epub 2019/06/18. doi: 10.1016/j.devcel.2019.05.024. PubMed PMID: 31204175.
3. Morata G, Ripoll P. Minutes: mutants of drosophila autonomously affecting cell division rate. Dev Biol. 1975;42(2):211-21. doi: 10.1016/0012-1606(75)90330-9. PubMed PMID: 1116643.
4. Meyer SN, Amoyel M, Bergantinos C, de la Cova C, Schertel C, Basler K, Johnston LA. An ancient defense system eliminates unfit cells from developing tissues during cell competition. Science. 2014;346(6214):1258236. doi: 10.1126/science.1258236. PubMed PMID: 25477468; PMCID: PMC5095928.
5. Alpar L, Bergantinos C, Johnston LA. Spatially Restricted Regulation of Spatzle/Toll Signaling during Cell Competition. Dev Cell. 2018. doi: 10.1016/j.devcel.2018.08.001. PubMed PMID: 30146479.
6. Byun PK, Zhang C, Yao B, Wardwell-Ozgo J, Terry D, Jin P, Moberg K. The Taiman Transcriptional Coactivator Engages Toll Signals to Promote Apoptosis and Intertissue Invasion in Drosophila. Curr Biol. 2019;29(17):2790-800 e4. Epub 2019/08/14. doi: 10.1016/j.cub.2019.07.012. PubMed PMID: 31402304; PMCID: PMC6736757.
7. Nagata R, Akai N, Kondo S, Saito K, Ohsawa S, Igaki T. Yorkie drives supercompetition by non-autonomous induction of autophagy via bantam microRNA in Drosophila. Curr Biol. 2022;32(5):1064-76 e4. Epub 2022/02/09. doi: 10.1016/j.cub.2022.01.016. PubMed PMID: 35134324.
8. Nagata R, Nakamura M, Sanaki Y, Igaki T. Cell Competition Is Driven by Autophagy. Dev Cell. 2019;51(1):99-112 e4. Epub 2019/09/24. doi: 10.1016/j.devcel.2019.08.018. PubMed PMID: 31543447.
9. Yamamoto M, Ohsawa S, Kunimasa K, Igaki T. The ligand Sas and its receptor PTP10D drive tumour-suppressive cell competition. Nature. 2017;542(7640):246-50. doi: 10.1038/nature21033.
10. Rhiner C, Lopez-Gay JM, Soldini D, Casas-Tinto S, Martin FA, Lombardia L, Moreno E. Flower forms an extracellular code that reveals the fitness of a cell to its neighbors in Drosophila. Dev Cell. 2010;18(6):985-98. Epub 2010/07/16. doi: 10.1016/j.devcel.2010.05.010. PubMed PMID: 20627080.
11. Portela M, Casas-Tinto S, Rhiner C, Lopez-Gay JM, Dominguez O, Soldini D, Moreno E. Drosophila SPARC is a self-protective signal expressed by loser cells during cell competition. Dev Cell. 2010;19(4):562-73. doi: 10.1016/j.devcel.2010.09.004. PubMed PMID: 20951347.
12. Merino MM, Rhiner C, Lopez-Gay JM, Buechel D, Hauert B, Moreno E. Elimination of unfit cells maintains tissue health and prolongs lifespan. Cell. 2015;160(3):461-76. Epub 2015/01/21. doi: 10.1016/j.cell.2014.12.017. PubMed PMID: 25601460; PMCID: PMC4313366.

13. Moreno E, Basler K, Morata G. Cells compete for decapentaplegic survival factor to prevent apoptosis in Drosophila wing development. Nature. 2002;416(6882):755-9. doi: 10.1038/416755a. PubMed PMID: 11961558.

14. Moreno E, Basler K. dMyc transforms cells into super-competitors. Cell. 2004;117(1):117-29. PubMed PMID: 15066287.

15. Zhang C, Robinson BS, Xu W, Yang L, Yao B, Zhao H, Byun PK, Jin P, Veraksa A, Moberg KH. The ecdysone receptor coactivator Taiman links Yorkie to transcriptional control of germline stem cell factors in somatic tissue. Dev Cell. 2015;34(2):168-80. doi: 10.1016/j.devcel.2015.05.010. PubMed PMID: 26143992; PMCID: PMC4519380.

16. Suijkerbuijk SJ, Kolahgar G, Kucinski I, Piddini E. Cell Competition Drives the Growth of Intestinal Adenomas in Drosophila. Current biology : CB. 2016;26(4):428-38. doi: 10.1016/j.cub.2015.12.043.

17. Vincent JP, Kolahgar G, Gagliardi M, Piddini E. Steep differences in wingless signaling trigger Myc-independent competitive cell interactions. Dev Cell. 2011;21(2):366-74. Epub 2011/08/16. doi: 10.1016/j.devcel.2011.06.021. PubMed PMID: 21839923; PMCID: PMC3209557.

18. Germani F, Hain D, Sternlicht D, Moreno E, Basler K. The Toll pathway inhibits tissue growth and regulates cell fitness in an infection-dependent manner. eLife. 2018;7. Epub 2018/11/20. doi: 10.7554/eLife.39939. PubMed PMID: 30451683; PMCID: PMC6279345.

19. Baker NE, Kiparaki M, Khan C. A potential link between p53, cell competition and ribosomopathy in mammals and in Drosophila. Dev Biol. 2019;446(1):17-9. Epub 2018/12/05. doi: 10.1016/j.ydbio.2018.11.018. PubMed PMID: 30513308; PMCID: PMC6642609.

20. de la Cova C, Senoo-Matsuda N, Ziosi M, Wu DC, Bellosta P, Quinzii CM, Johnston LA. Supercompetitor status of Drosophila Myc cells requires p53 as a fitness sensor to reprogram metabolism and promote viability. Cell Metab. 2014;19(3):470-83. Epub 2014/02/25. doi: 10.1016/j.cmet.2014.01.012. PubMed PMID: 24561262; PMCID: PMC3970267.

21. Merino MM, Seum C, Dubois M, Gonzalez-Gaitan M. A role for Flower and cell death in controlling morphogen gradient scaling. Nat Cell Biol. 2022;24(4):424-33. Epub 2022/03/19. doi: 10.1038/s41556-022-00858-3. PubMed PMID: 35301437.

22. Boulan L, Andersen D, Colombani J, Boone E, Leopold P. Inter-Organ Growth Coordination Is Mediated by the Xrp1-Dilp8 Axis in Drosophila. Dev Cell. 2019;49(5):811-8 e4. Epub 2019/04/23. doi: 10.1016/j.devcel.2019.03.016. PubMed PMID: 31006647.

23. Xu D, Woodfield SE, Lee TV, Fan Y, Antonio C, Bergmann A. Genetic control of programmed cell death (apoptosis) in Drosophila. Fly (Austin). 2009;3(1):78-90. Epub 2009/02/03. doi: 10.4161/fly.3.1.7800. PubMed PMID: 19182545; PMCID: PMC2702463.

24. Wang C, Yin M-X, Wu W, Dong L, Wang S, Lu Y, Xu J, Wu W, Li S, Zhao Y, Zhang L. Taiman acts as a coactivator of Yorkie in the Hippo pathway to promote tissue growth and intestinal regeneration. Cell Discovery. 2016;2:16006. doi: 10.1038/celldisc.2016.6 http://www.nature.com/articles/celldisc20166#supplementary-information.

25. Huang J, Wu S, Barrera J, Matthews K, Pan D. The Hippo signaling pathway coordinately regulates cell proliferation and apoptosis by inactivating Yorkie, the

Drosophila Homolog of YAP. Cell. 2005;122(3):421-34. doi: S0092-8674(05)00552-0 [pii]10.1016/j.cell.2005.06.007. PubMed PMID: 16096061.

26. Tripathi BK, Irvine KD. The wing imaginal disc. Genetics. 2022;220(4). Epub 2022/03/05. doi: 10.1093/genetics/iyac020. PubMed PMID: 35243513; PMCID: PMC8982031.

27. Zeng W, Wharton KA, Jr., Mack JA, Wang K, Gadbaw M, Suyama K, Klein PS, Scott MP. naked cuticle encodes an inducible antagonist of Wnt signalling. Nature. 2000;403(6771):789-95. Epub 2000/02/29. doi: 10.1038/35001615. PubMed PMID: 10693810.

28. Rulifson EJ, Micchelli CA, Axelrod JD, Perrimon N, Blair SS. wingless refines its own expression domain on the Drosophila wing margin. Nature. 1996;384(6604):72-4. Epub 1996/11/07. doi: 10.1038/384072a0. PubMed PMID: 8900280.

29. Baeg GH, Selva EM, Goodman RM, Dasgupta R, Perrimon N. The Wingless morphogen gradient is established by the cooperative action of Frizzled and Heparan Sulfate Proteoglycan receptors. Dev Biol. 2004;276(1):89-100. Epub 2004/11/09. doi: 10.1016/j.ydbio.2004.08.023. PubMed PMID: 15531366.

30. Kirkpatrick CA, Dimitroff BD, Rawson JM, Selleck SB. Spatial regulation of Wingless morphogen distribution and signaling by Dally-like protein. Dev Cell. 2004;7(4):513-23. Epub 2004/10/08. doi: 10.1016/j.devcel.2004.08.004. PubMed PMID: 15469840.

31. Han C, Yan D, Belenkaya TY, Lin X. Drosophila glypicans Dally and Dally-like shape the extracellular Wingless morphogen gradient in the wing disc. Development. 2005;132(4):667-79. Epub 2005/01/14. doi: 10.1242/dev.01636. PubMed PMID: 15647319.

32. Franch-Marro X, Wendler F, Griffith J, Maurice MM, Vincent JP. In vivo role of lipid adducts on Wingless. J Cell Sci. 2008;121(Pt 10):1587-92. Epub 2008/04/24. doi: 10.1242/jcs.015958. PubMed PMID: 18430784; PMCID: PMC7611555.

33. Tang X, Wu Y, Belenkaya TY, Huang Q, Ray L, Qu J, Lin X. Roles of N-glycosylation and lipidation in Wg secretion and signaling. Dev Biol. 2012;364(1):32-41. Epub 2012/01/31. doi: 10.1016/j.ydbio.2012.01.009. PubMed PMID: 22285813; PMCID: PMC3315154.

34. Norman M, Vuilleumier R, Springhorn A, Gawlik J, Pyrowolakis G. Pentagone internalises glypicans to fine-tune multiple signalling pathways. eLife. 2016;5. Epub 2016/06/09. doi: 10.7554/eLife.13301. PubMed PMID: 27269283; PMCID: PMC4924993.

35. Uyehara CM, McKay DJ. Direct and widespread role for the nuclear receptor EcR in mediating the response to ecdysone in Drosophila. Proc Natl Acad Sci U S A. 2019;116(20):9893-902. Epub 2019/04/26. doi: 10.1073/pnas.1900343116. PubMed PMID: 31019084; PMCID: PMC6525475.

36. Yan D, Wu Y, Feng Y, Lin SC, Lin X. The core protein of glypican Dally-like determines its biphasic activity in wingless morphogen signaling. Dev Cell. 2009;17(4):470-81. Epub 2009/10/27. doi: 10.1016/j.devcel.2009.09.001. PubMed PMID: 19853561; PMCID: PMC3326419.

37. Strigini M, Cohen SM. Wingless gradient formation in the Drosophila wing. Curr Biol. 2000;10(6):293-300. Epub 2000/04/04. doi: 10.1016/s0960-9822(00)00378-x. PubMed PMID: 10744972.

38. Zeng X, Han L, Singh SR, Liu H, Neumuller RA, Yan D, Hu Y, Liu Y, Liu W, Lin X, Hou SX. Genome-wide RNAi screen identifies networks involved in intestinal stem cell regulation in Drosophila. Cell reports. 2015;10(7):1226-38. Epub 2015/02/24. doi: 10.1016/j.celrep.2015.01.051. PubMed PMID: 25704823; PMCID: PMC4420031.

39. Bai J, Uehara Y, Montell DJ. Regulation of invasive cell behavior by taiman, a Drosophila protein related to AIB1, a steroid receptor coactivator amplified in breast cancer. Cell. 2000;103(7):1047-58. Epub 2001/02/13. PubMed PMID: 11163181.

40. Bejsovec A. Wingless Signaling: A Genetic Journey from Morphogenesis to Metastasis. Genetics. 2018;208(4):1311-36. Epub 2018/04/06. doi: 10.1534/genetics.117.300157. PubMed PMID: 29618590; PMCID: PMC5887133.

41. Su TY, Nakato E, Choi PY, Nakato H. Drosophila Glypicans Regulate Follicle Stem Cell Maintenance and Niche Competition. Genetics. 2018;209(2):537-49. Epub 2018/04/11. doi: 10.1534/genetics.118.300839. PubMed PMID: 29632032; PMCID: PMC5972425.

42. Yi P, Wang Z, Feng Q, Pintilie GD, Foulds CE, Lanz RB, Ludtke SJ, Schmid MF, Chiu W, O'Malley BW. Structure of a biologically active estrogen receptor-coactivator complex on DNA. Mol Cell. 2015;57(6):1047-58. Epub 2015/03/03. doi: 10.1016/j.molcel.2015.01.025. PubMed PMID: 25728767; PMCID: PMC4369429.

43. Regan JC, Brandão AS, Leitão AB, Dias Â, Sucena É, Jacinto A, Zaidman-Rémy A. Steroid Hormone Signaling Is Essential to Regulate Innate Immune Cells and Fight Bacterial Infection in Drosophila. PLoS Pathogens. 2013;9(10). doi: 10.1371/journal.ppat.1003720.

44. Parker J, Struhl G. Control of Drosophila wing size by morphogen range and hormonal gating. Proc Natl Acad Sci U S A. 2020;117(50):31935-44. Epub 2020/12/02. doi: 10.1073/pnas.2018196117. PubMed PMID: 33257577; PMCID: PMC7749314.

45. Mitchell NC, Lin JI, Zaytseva O, Cranna N, Lee A, Quinn LM. The Ecdysone receptor constrains wingless expression to pattern cell cycle across the Drosophila wing margin in a Cyclin B-dependent manner. BMC Dev Biol. 2013;13:28. Epub 2013/07/16. doi: 10.1186/1471-213X-13-28. PubMed PMID: 23848468; PMCID: PMC3720226.

46. Witte L, Linnemannstons K, Honemann-Capito M, Gross JC. Visualization and Quantitation of Wg trafficking in the Drosophila Wing Imaginal Epithelium. Bio Protoc. 2021;11(11):e4040. Epub 2021/07/13. doi: 10.21769/BioProtoc.4040. PubMed PMID: 34250206; PMCID: PMC8250385.

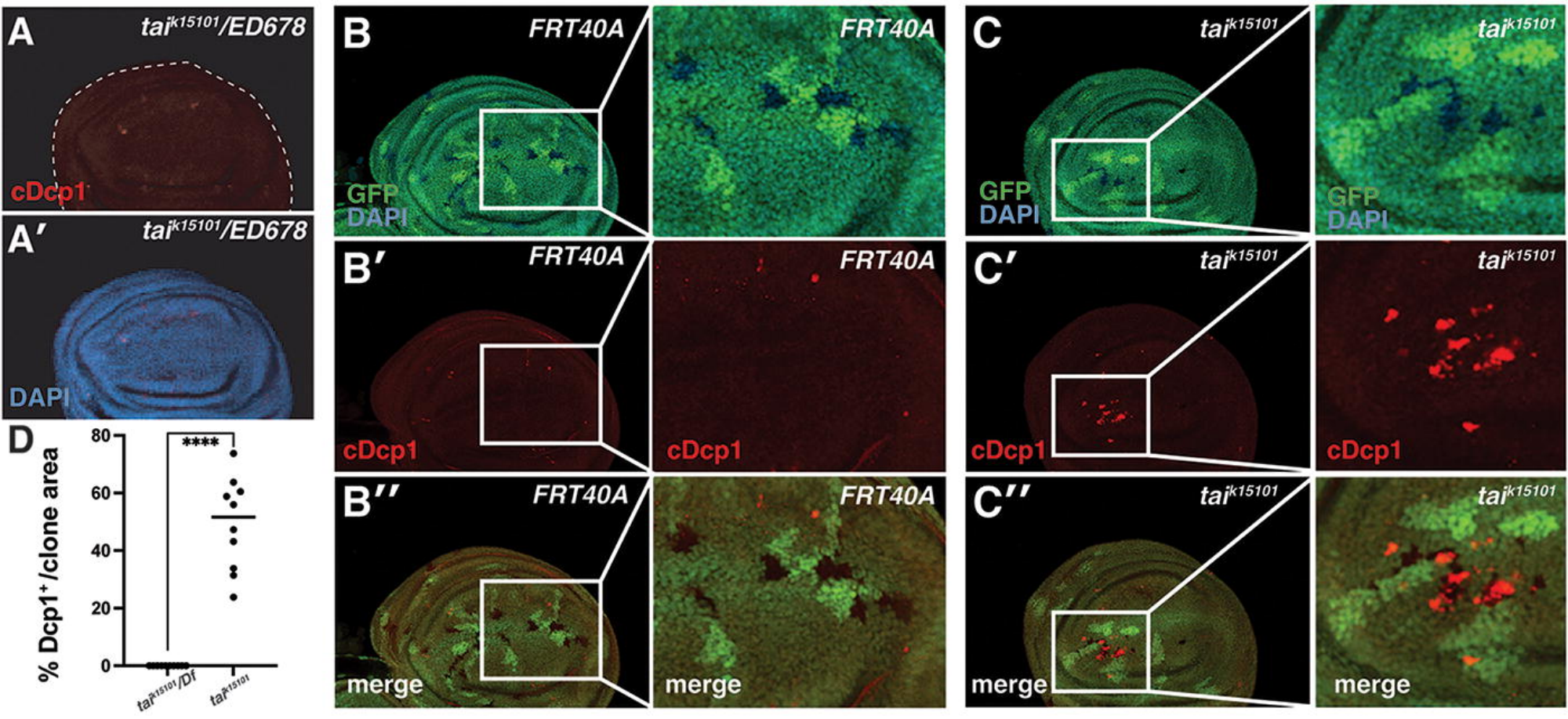
A
tai^{k15101}/ED678
cDcp1
A′
tai^{k15101}/ED678
DAPI
B
FRT40A
GFP
DAPI
FRT40A
B′
FRT40A
cDcp1
FRT40A
cDcp1
B″
FRT40A
merge
FRT40A
merge
C
tai^{k15101}
GFP
DAPI
tai^{k15101}
GFP
DAPI
C′
tai^{k15101}
cDcp1
tai^{k15101}
cDcp1
C″
tai^{k15101}
merge
tai^{k15101}
merge
D
% Dcp1^{+}/clone area
80
60
40
20
0
****
tai^{k15101}/Df
tai^{k15101}

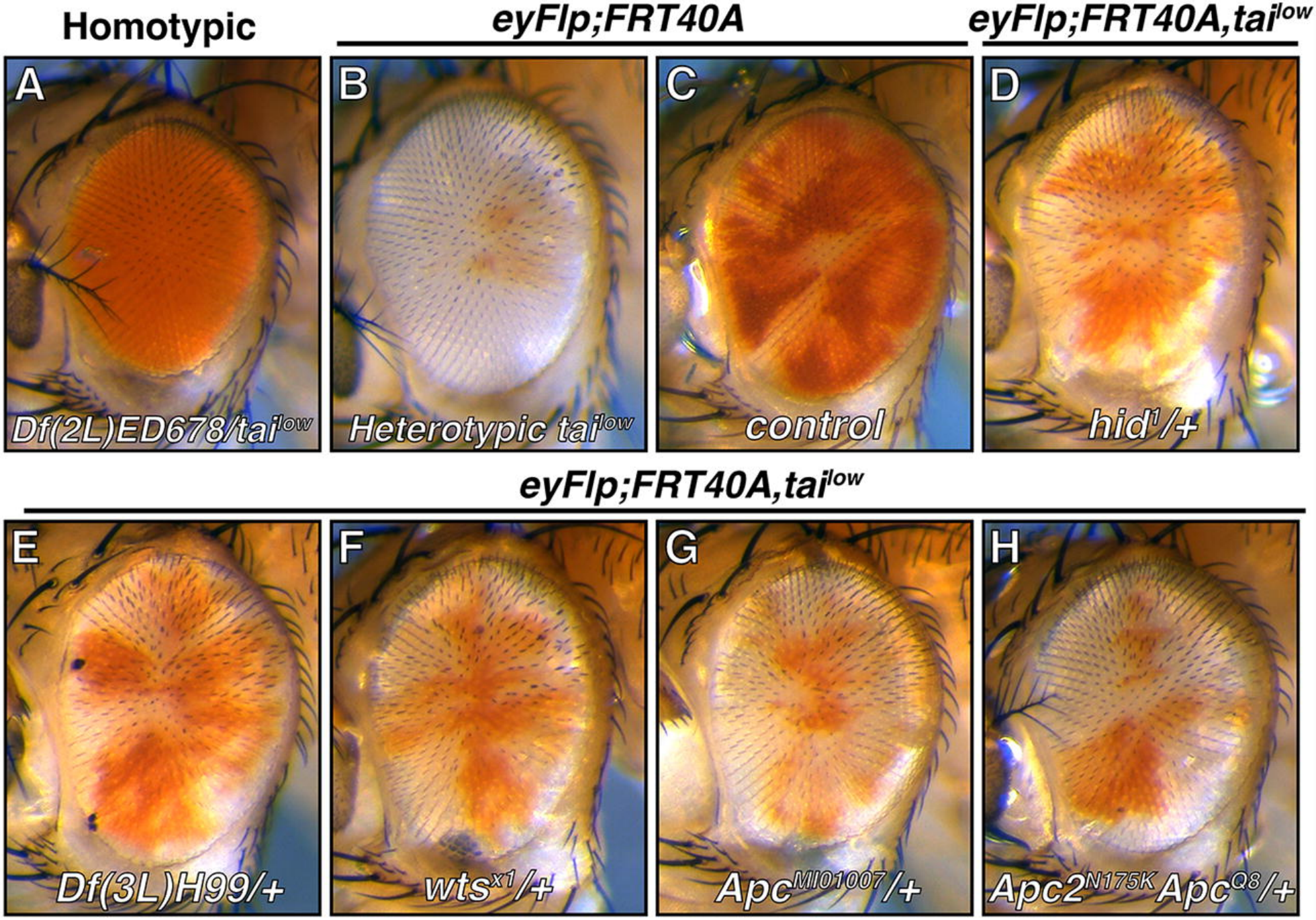
Homotypic
eyFlp;FRT40A
eyFlp;FRT40A,tai^low
A
Df(2L)ED678/tai^low
B
Heterotypic tai^low
C
control
D
hid^1/+
eyFlp;FRT40A,tai^low
E
Df(3L)H99/+
F
wts^x1/+
G
Apc^MI01007/+
H
Apc2^N175K Apc^Q8/+

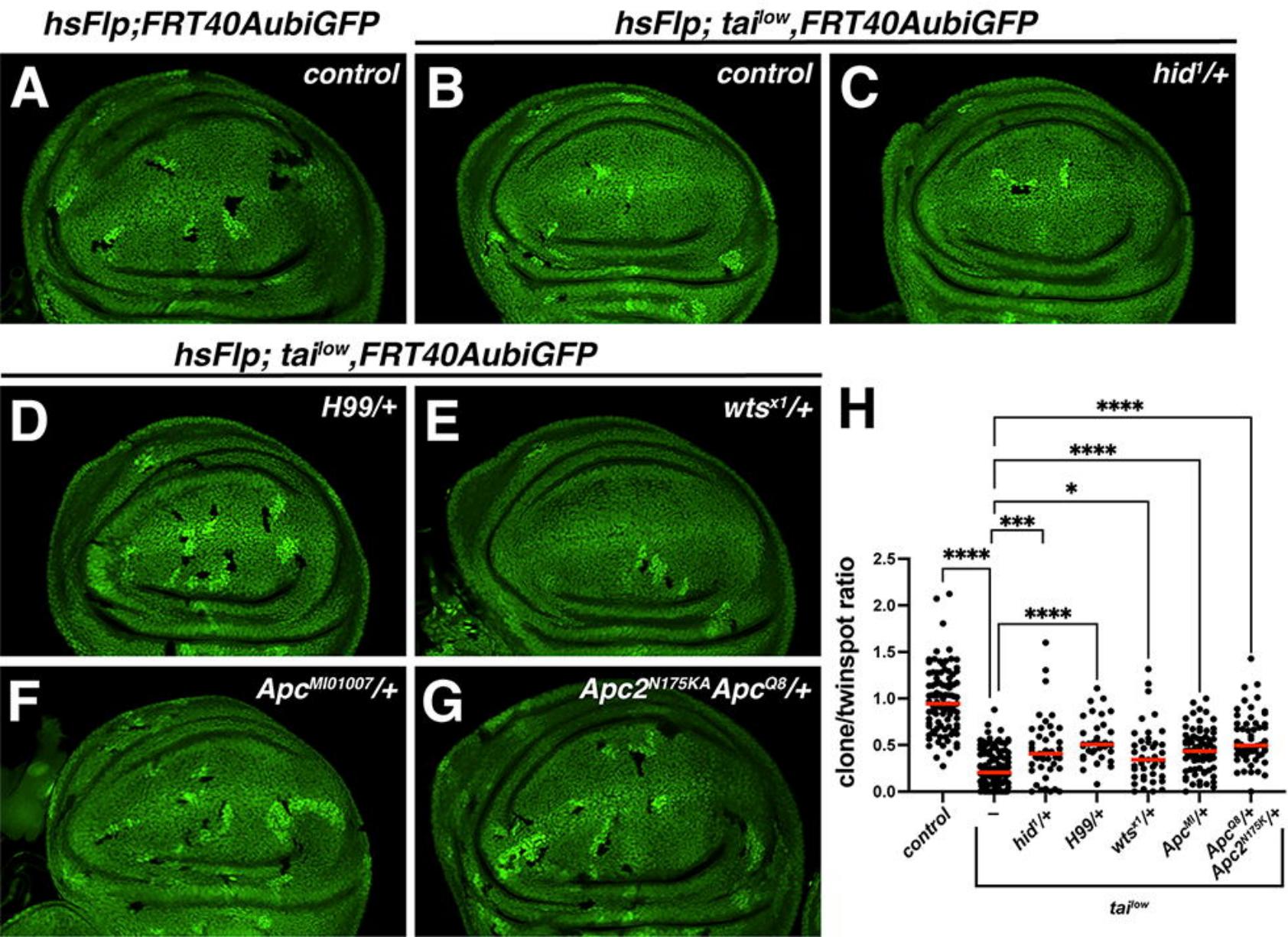
hsFlp;FRT40AubiGFP
hsFlp; tai^low,FRT40AubiGFP
A
control
B
control
C
hid^1/+
hsFlp; tai^low,FRT40AubiGFP
D
H99/+
E
wts^x1/+
F
Apc^MI01007/+
G
Apc2^N175KA Apc^Q8/+
H
clone/twinspot ratio
2.5
2.0
1.5
1.0
0.5
0.0
****
***
*
control
–
hid^1/+
H99/+
wts^x1/+
Apc^MI/+
Apc^Q8/+
Apc2^N175K/+
tai^low

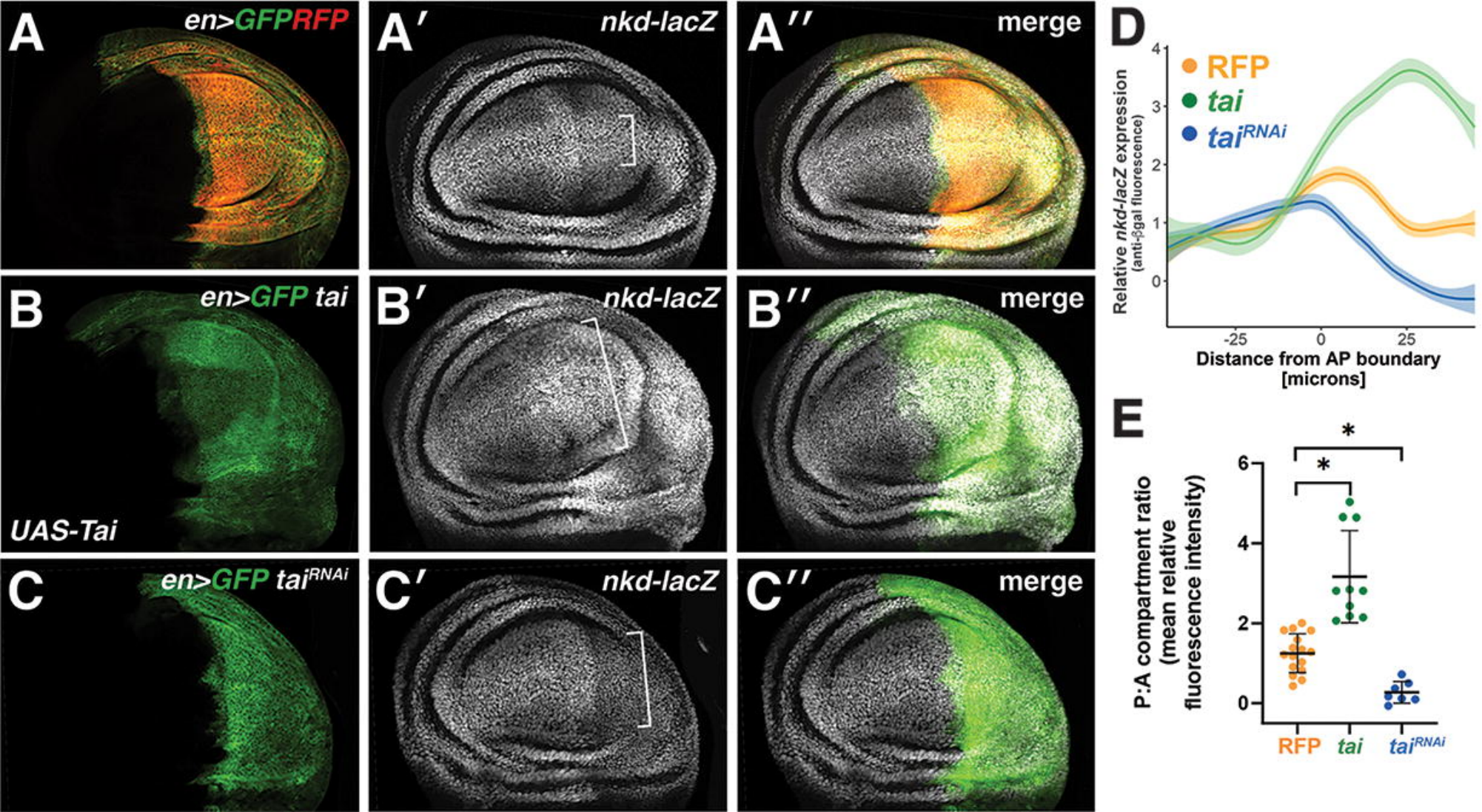
A
en>GFPRFP
A′
nkd-lacZ
A″
merge
B
en>GFP tai
UAS-Tai
B′
nkd-lacZ
B″
merge
C
en>GFP taiRNAi
C′
nkd-lacZ
C″
merge
D
RFP
tai
taiRNAi
Relative nkd-lacZ expression
(anti-βgal fluorescence)
4
3
2
1
0
-25
0
25
Distance from AP boundary
[microns]
E
P:A compartment ratio
(mean relative
fluorescence intensity)
6
4
2
0
*
*
RFP
tai
taiRNAi

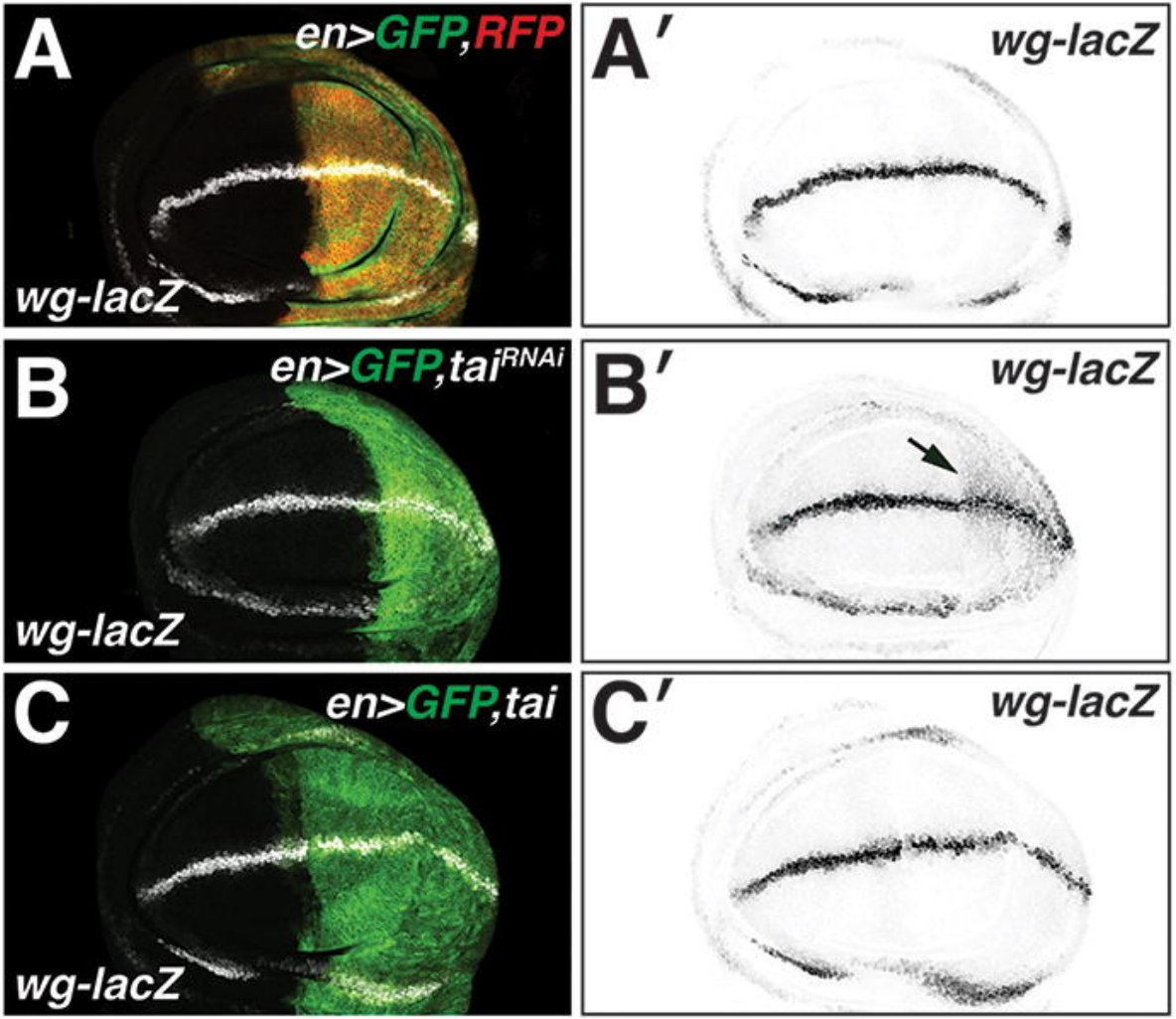
A
en>GFP,RFP
wg-lacZ
A′
wg-lacZ
B
en>GFP,tai^RNAi
wg-lacZ
B′
wg-lacZ
C
en>GFP,tai
wg-lacZ
C′
wg-lacZ

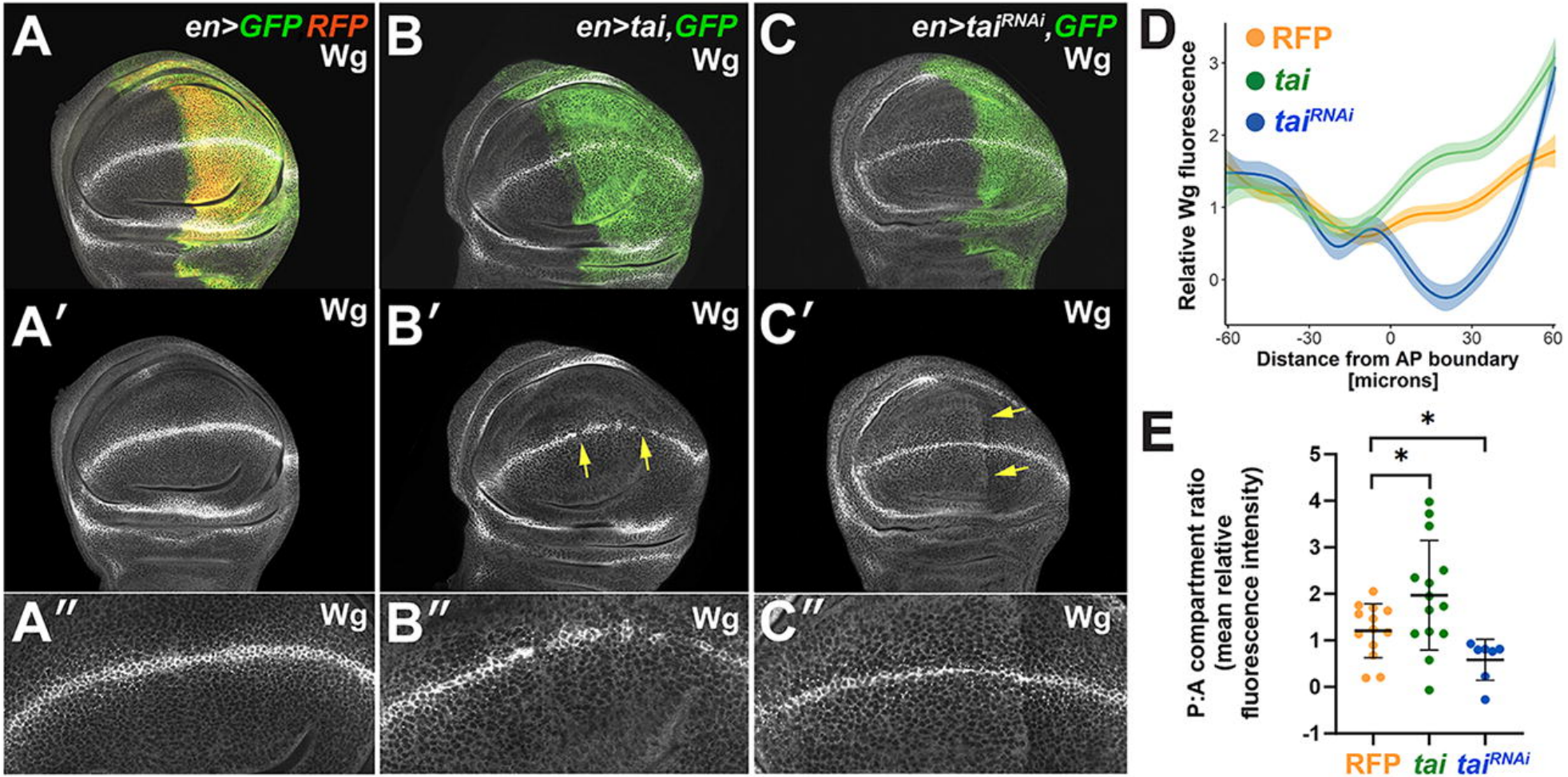
A
en>GFP RFP
Wg
B
en>tai,GFP
Wg
C
en>tai^RNAi,GFP
Wg
A′
Wg
B′
Wg
C′
Wg
A″
Wg
B″
Wg
C″
Wg
D
RFP
tai
tai^RNAi
Relative Wg fluorescence
Distance from AP boundary [microns]
-60
-30
0
30
60
E
P:A compartment ratio (mean relative fluorescence intensity)
*
*
RFP
tai
tai^RNAi

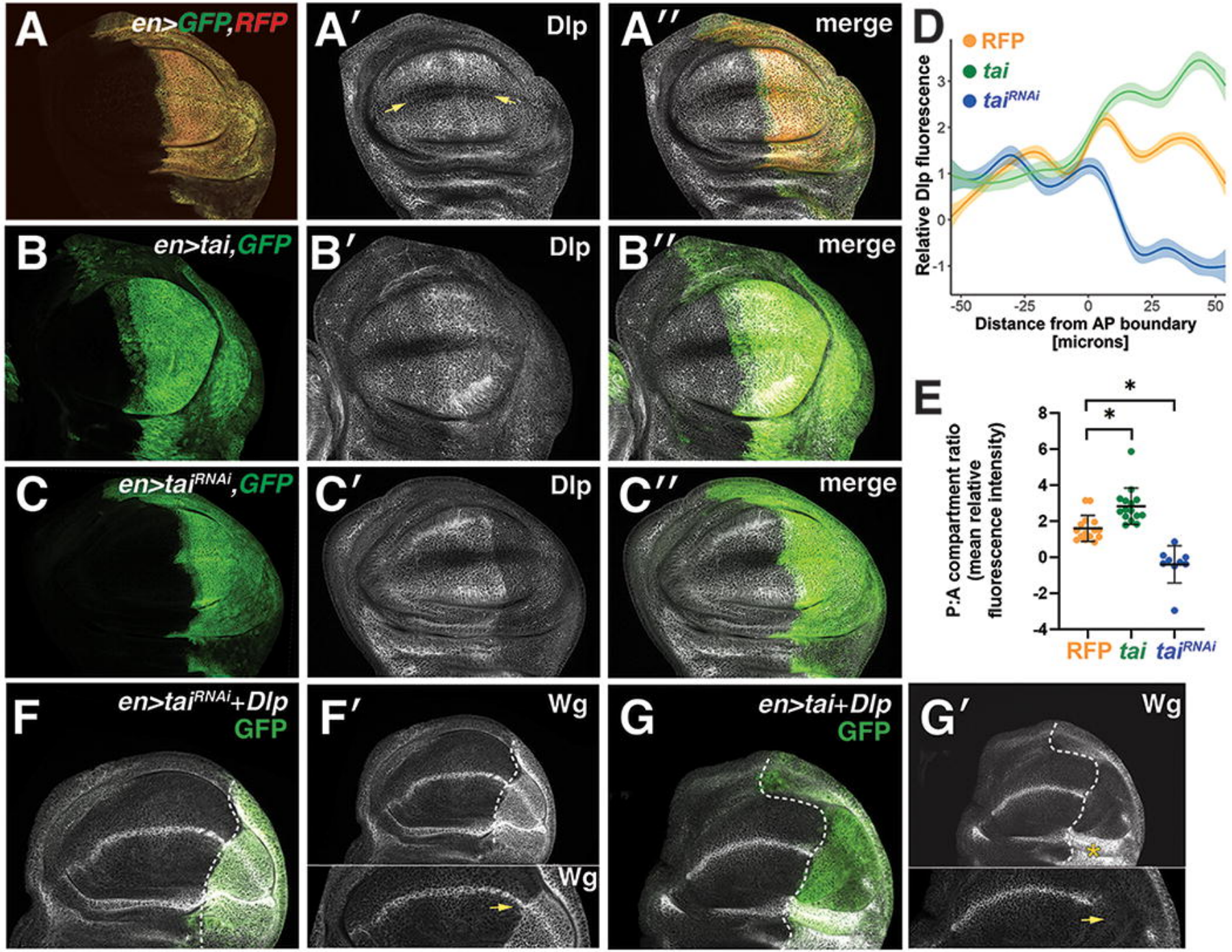
A
en>GFP,RFP
A′
Dlp
A″
merge
B
en>tai,GFP
B′
Dlp
B″
merge
C
en>tai^RNAi,GFP
C′
Dlp
C″
merge
D
RFP
tai
tai^RNAi
Relative Dlp fluorescence
Distance from AP boundary [microns]
E
P:A compartment ratio (mean relative fluorescence intensity)
RFP
tai
tai^RNAi
F
en>tai^RNAi+Dlp
GFP
F′
Wg
Wg
G
en>tai+Dlp
GFP
G′
Wg

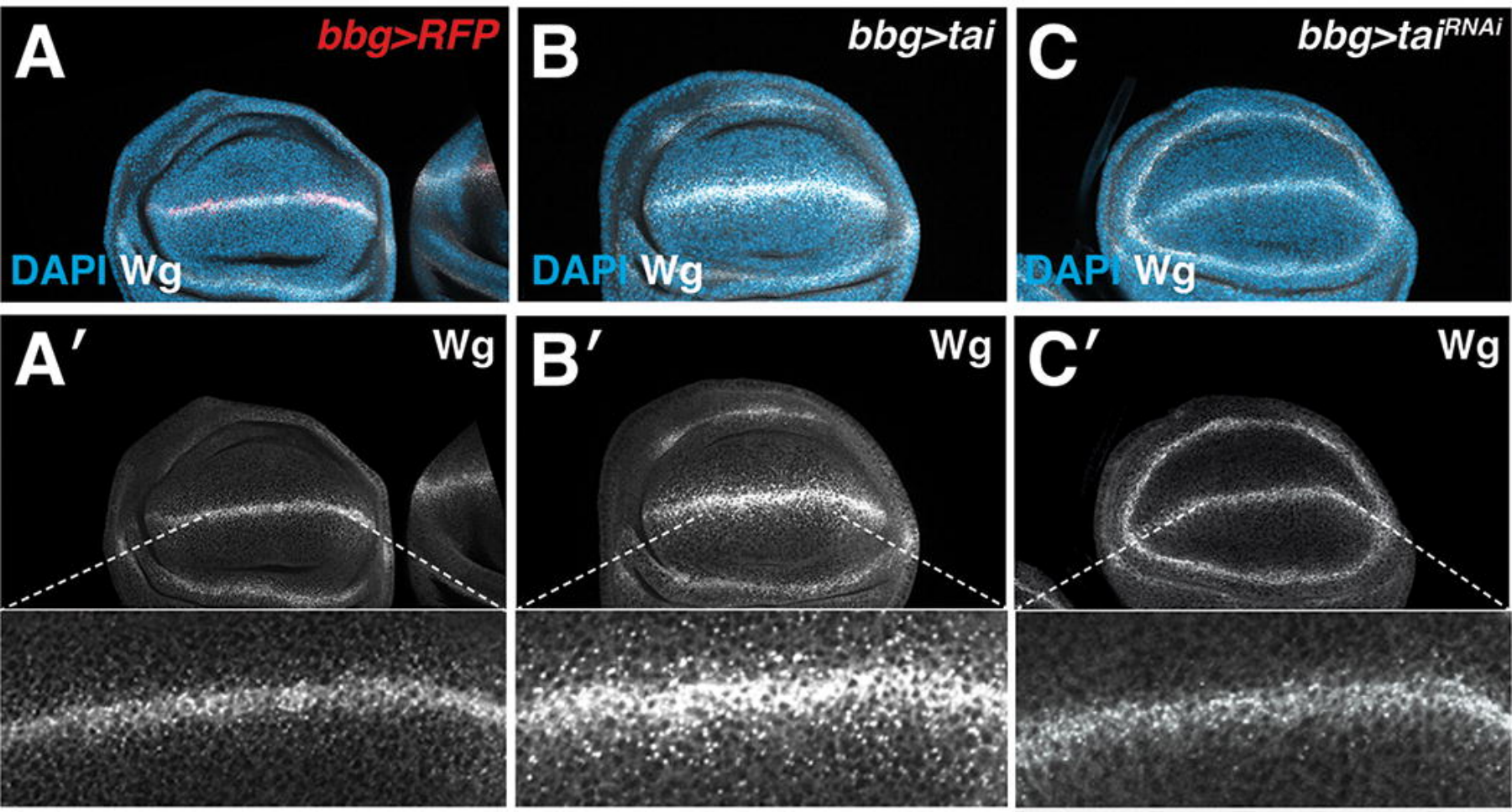
A
bbg>RFP
DAPI Wg
B
bbg>tai
DAPI Wg
C
bbg>tai^RNAi
DAPI Wg
A′
Wg
B′
Wg
C′
Wg

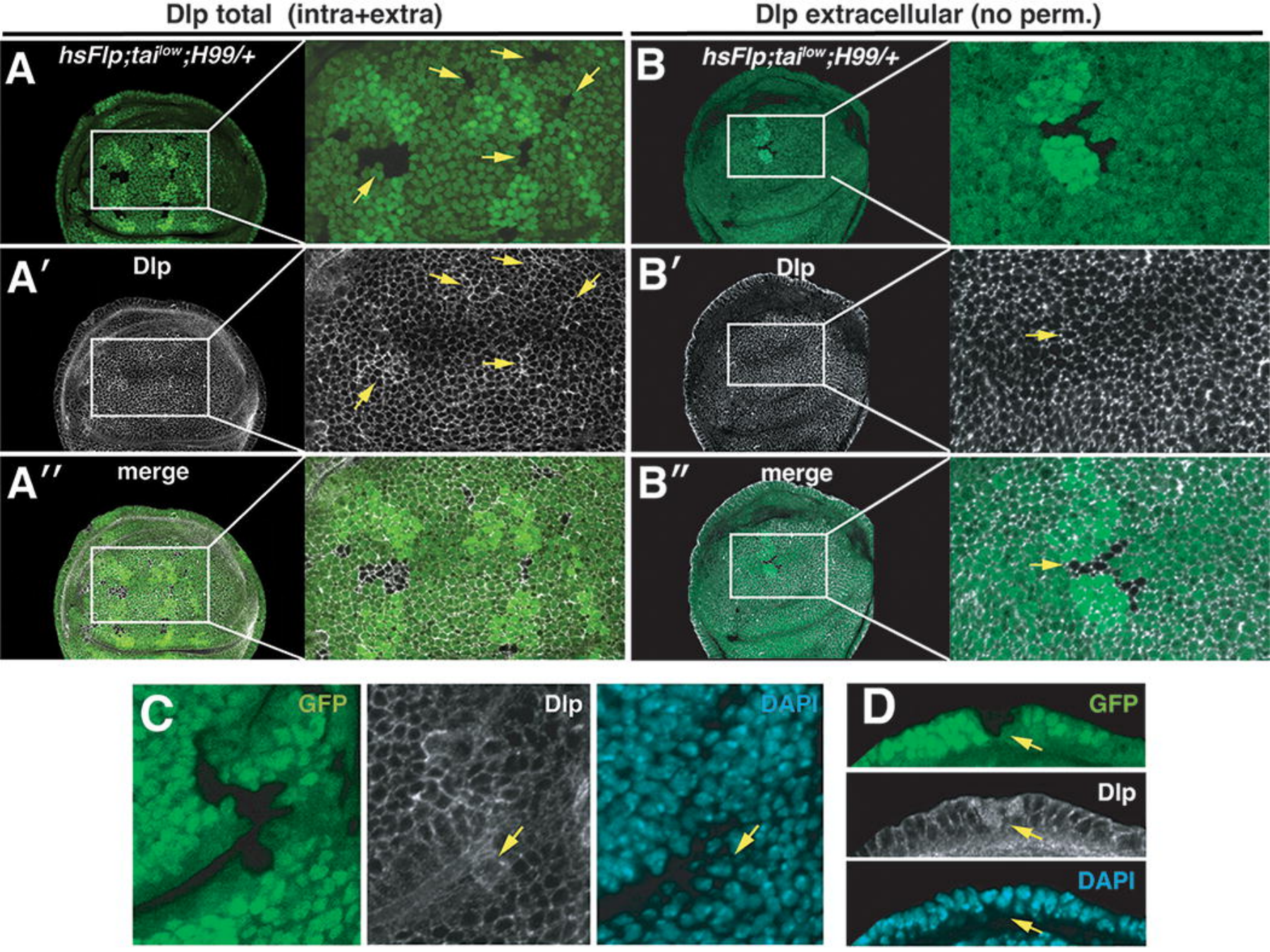
Dlp total (intra+extra)
Dlp extracellular (no perm.)
A
hsFlp;tai^low;H99/+
B
hsFlp;tai^low;H99/+
A′
Dlp
B′
Dlp
A″
merge
B″
merge
C
GFP
Dlp
DAPI
D
GFP
Dlp
DAPI